JOURNAL OF CATALYSIS 123, 98–112 (1990)

The Formation of Supported Bimetallic Catalysts

I. The Measurement of Enthalpies of Gas–Solid Reactions Using Differential Scanning Calorimetry

BAHMAN REJAI[1] AND RICHARD D. GONZALEZ[2]

Department of Chemical Engineering, University of Illinois at Chicago, Box 4348, Chicago, Illinois 60680

Received February 16, 1989; revised December 12, 1989

Thermal analysis techniques suffer from the lack of reproducibility and are difficult to quantify. This study addresses the significant variables responsible for these drawbacks and explores the possibility of the precise determination of the enthalpy of a desired reaction using differential scanning calorimetry (DSC). A method in which the significant experimental variables are extrapolated is proposed for two types of gas–solid reactions of interest to catalysis. The reduction of PtO_2 and $PtCl_2$, in addition to the decomposition of calcium oxalate, is reported. The method successfully yields enthalpies of reaction which are in agreement with enthalpies calculated from heats of formation reported in the literature. © 1990 Academic Press, Inc.

INTRODUCTION

The process of catalyst reduction and activation is undoubtedly significant in catalysis as it has implications for the structure and morphology of the resulting catalyst. The morphology, in turn, controls both the activity and performance of the catalyst.

In catalyst characterization studies, various techniques are currently used to study the kinetics and the mechanism by which the reduction process occurs. Among these, temperature-programmed (TP) techniques are of particular interest. These techniques are generally based on the measurement of compositional changes in gaseous reactants or products as a function of catalyst temperature. The heat liberated during reaction is, of course, dependent on the particular phase change or reaction involved. These techniques have been used primarily as qualitative tools and give little or no quantitative information regarding enthalpies of the reactions involved. Another drawback to the use of conventional TP techniques is the lack of reproducibility from one laboratory to another or even from one experiment to the next. This may arise from the vulnerability to artifacts caused by heat or mass transfer effects, which are generally overlooked. This study attempts to clarify the effect of these artifacts and to explore the feasibility of the quantitative determination of the enthalpy of a desired reaction using differential scanning calorimetry (DSC). Although some investigators (*1*) have measured heats of adsorption of several gases on supported metal catalysts, the enthalpies of gas–solid reactions such as reductions or decompositions using DSC have not yet been reported.

REVIEW OF THERMAL ANALYSIS: CAPABILITIES AND APPLICATIONS

Subsequent to their development, thermal analysis techniques (TA) have been used in preference to the older adiabatic calorimetric devices, which were usually operated under isothermal conditions. The advantages of TA techniques include: speed

[1] Present address: Solar Energy Research Institute, Golden, CO.

[2] To whom correspondence should be addressed.

0021-9517/90 $3.00

and simplicity of operation, small sample size requirements, and convenience. Unfortunately, a disadvantage commonly encountered is the difficulty of quantifying the results. TA techniques have found widespread application in areas as diverse as quality control in pharmaceuticals (*2*) and materials science and polymers (*3–6*). Among the TA techniques, the two that have the potential for providing enthalpy information are differential thermal analysis (DTA) and differential scanning calorimetry (DSC). In a conventional DTA apparatus, the difference in temperature between a sample cell and an inert reference cell is measured as a function of either temperature or time, as the temperature is increased at a constant rate. The integrated area under a specific peak of the resulting exotherm or endotherm should be proportional to the enthalpy corresponding to that transition. In this technique, the proportionality constant relating peak areas to enthalpies is a function of temperature. DSC was first used by Watson *et al.* (*7*) and was designed to measure the differential electrical power required to maintain both the sample and reference holders at the same temperature while both are heated at a constant rate. Unlike DTA, the conversion of peak area to heat either evolved or absorbed during a transition, as measured by DSC, involves a single electrical conversion factor. This conversion factor is independent of temperature and other experimental conditions and, therefore, DSC can be used to measure enthalpies directly.

A large number of theoretical and empirical approaches have been employed in an attempt to quantify results of DTA. These studies have proved to be unsuccessful in accurately quantifying experimental results. An in-depth study which deals with the effect of the relevant experimental variables such as heating rate, sample size, and dilution has been performed by van Dooren and Muller (*8*). They concluded that these effects could not be systematically quantified. A series of DTA measurements performed on a variety of different samples were analyzed by De Bruijin and Marel (*9*). They concluded that DTA could not be used for precise quantitative analysis. Boersma (*10*) pointed out that due to the dependence of the proportionality constant on apparent sample density and sample thermal conductivity, quantitative DTA using conventional methods was inherently impossible. Ozawa (*11*), on the other hand, published a new simple and convenient technique by which DTA results could be quantified. This technique was based on the consideration of temperature gradients within the sample. An analytical evaluation of the DSC method was given by J. H. Flynn (*12*). He concluded that corrections for various instrumental time constants were required in order to obtain meaningful results. He also asserted that DSC can be used to determine enthalpies of phase transitions to an accuracy of within 1% when the baseline is unambiguous. A theoretical analysis of peak heights obtained using both DTA and DSC was given by Saito *et al.* (*13*). These authors reported that the limiting peak height obtained at an infinite heating rate was independent of the amount of sample and could be related to reaction enthalpies. The analysis of gas–solid reactions was first performed by Stone (*14*), who studied the effect of pressure and atmosphere on DTA using a dynamic gas technique. In a recent study, Chou and Vannice (*1*) measured the heats of adsorption of H_2 and CO on unsupported and supported Pd catalysts.

THE BASIC HEAT TRANSFER EQUATIONS GOVERNING DSC

Theoretical treatments of both DTA and DSC have been reported by several research groups (*10, 15–18*). A treatment related to the measurement of reaction enthalpies is presented here.

The heat transfer parts of a typical DSC consist of a sample and its holder at a temperature T_s, a source of thermal energy at a temperature T_p, and an intermediate region characterized by a thermal resistance R

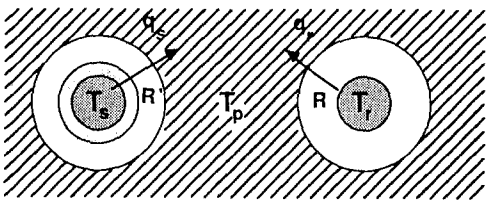

FIG. 1. Heat transfer parts of a DSC. A boundary layer of evolved gas introduces additional resistance on the sample side.

(Fig. 1). Energy flows to or from the sample at a rate dq_s/dt. At energy balance over the system requires that at any instant energy generated by the sample, dh/dt, either increases the sample temperature or is dissipated to the surroundings. This may be mathematically expressed as

$$\frac{dh}{dt} = C_s \frac{dT_s}{dt} - \frac{dq_s}{dt}, \tag{1}$$

where C_s is the heat capacity of the sample and its pan. Furthermore, the rate of heat loss to the surroundings may be expressed by Newton's law of cooling, i.e.,

$$\frac{dq_s}{dt} = \frac{T_s - T_p}{R}. \tag{2}$$

Taking the derivative with respect to time and rearranging yields

$$\frac{dT_s}{dt} = \frac{dT_p}{dt} - R\frac{d^2q_s}{dt^2}. \tag{3}$$

The combination of Eqs. (1) and (3) results in

$$\frac{dh}{dt} = C_s\left(\frac{dT_p}{dt} - R\frac{d^2q_s}{dt^2}\right) - \frac{dq_s}{dt}. \tag{4}$$

After writing similar equations for the reference side, for which $dh/dt = 0$, and subtracting it from the sample side, the equation

$$\frac{dh}{dt} = -\frac{dq}{dt} + (C_s - C_r)\frac{dT_p}{dt} - RC_s\frac{d^2q}{dt^2} \tag{5}$$

I II III

is obtained, where C_r is the heat capacity of the reference pan and $q = q_r - q_s$ is the net heat flow. It follows that dh/dt consists of three terms, the first term being the signal measured from the baseline, the second term being the baseline displacement due to the heat capacity difference between the sample and the reference, and the third term being the slope of the curve multiplied by a constant RC_s. This equation suggests that the area under a DSC peak is directly equal to the enthalpy change, ΔH, provided that the following conditions are met:

(1) The sample temperature, T_s, is uniform throughout the sample. This condition is satisfied when the sample is small or when it is a very good thermal conductor.

(2) The thermal resistance of the intermediate region, R, is the same for both the sample and the reference.

(3) Both C_s and R are constant over the temperature range used.

EXPERIMENTAL

Materials and supplies. PtO_2(85.91% Pt) and $PtCl_2$(73.21% Pt) were purchased from Strem Chemicals (Newburyport, MA). The $CaC_2O_4 \cdot H_2O$ was obtained from Fisher Scientific Co. (Fair Lawn, NJ). Gases were all ultrahigh purity grade and were purchased from the Linox Co. (Hillside, IL). They were subjected to further purification by passing them through an oxygen trap (Supelco) and a molecular sieve which was cooled by means of a dry ice/acetone bath.

Differential scanning calorimeter. A commercial Perkin–Elmer DSC-7 calorimeter was modified for continuous flow operation as follows: (1) The gases were mixed and the total purge gas flow rate was controlled using electronic flow controllers (Tylan Corp., Carson, CA); (2) the sample and reference outlet lines were separated and similar flow rates were obtained through the use of adjustable needle valves, and (3) the Pt sample pan covers were perforated and the aluminum covers discarded in order to obtain a better gas–solid contact.

Calibrations for temperature and enthalpy were performed using the melting transitions of indium and zinc standards. An

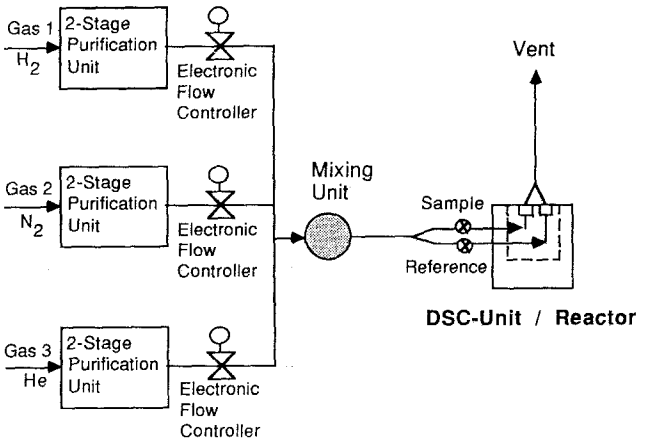

FIG. 2. Diagram of the gas flow system.

empty aluminum pan was placed in the reference cavity for each reduction experiment. A dehydrated calcium oxalate sample was used as the reference for the dehydration experiments. Weight changes upon reduction or decomposition were recorded using a Sartorius electronic microbalance which had a precision of 0.1 mg or an accuracy of 0.05 mg. The values of temperature and enthalpy for each experimental data point reported is the average of three runs under identical conditions. The error bars on graphs indicate the margin for a 99% confidence level, i.e., $x = \mu \pm 3\sigma$.

A diagram of the DSC and the associated flow system is shown in Fig. 2.

RESULTS AND DISCUSSION

In order to quantify enthalpies of reaction, two types of gas–solid reactions were studied:

(*1*) *Decomposition.* In this case, the sample is decomposed or dehydrated upon heating. This results in the evolution of gaseous products which form a boundary layer around the sample. The thermal conductivity of the intermediate region, with respect to that of the reference side, is changed as a result of the formation of this boundary layer (Fig. 1).

(*2*) *Reduction.* In this case the purge gas contains hydrogen, which is consumed during the reaction. Additionally, a gaseous product such as water or hydrogen chloride is evolved. The change in the thermal conductivity of the intermediate purge gas region occurs as the result of both the consumption of hydrogen and the evolution of gaseous products.

In both types of reactions a dissimilarity between the thermal resistance of the sample and the reference is created. This dissimilarity can be particularly large when the thermal conductivity of the purge gas (helium, for example) is significantly different from that of the gaseous products evolved (*1*). Thermal conductivities of several gases of interest are shown in Table 1 (*19*). Because the thermal conductivities of N_2 and Ar are reasonably close to that of water, the use of either of these purge gases represents a good choice when water is a reaction product.

In measuring enthalpies for dehydration reactions, accurate values will be obtained only when ideal conditions, as outlined above, are approached. This suggests that (1) the sample temperature, T_s, must be uniform and that, (2) the thermal conductivity of the purge gas should be equal to that of the evolved gas. Under these conditions, the thermal resistance, R, for the sample

TABLE I
Thermal Conductivities of Some Gases at Room Temperature (25°C) in W/(m K) (Ref. (19))

Gas	Thermal conductivity (W/(m K))
H_2	0.1750
He	0.1470
O_2	0.0263
N_2	0.0255
CO	0.0248
H_2O	0.0179
Ar	0.0174
CO_2	0.0169
HCl	0.0148
Cl_2	0.0092

side will approach that of the reference side and Eq. (5) will be valid. Two sets of experiments were performed to test this hypothesis:

(1) The dehydration temperature, T, and the enthalpy change, ΔH, were measured using different sample sizes and the results were extrapolated to zero sample size.

(2) The dehydration temperature, T, and the enthalpy change, ΔH, were measured using purge gases with different thermal conductivities. The results were extrapolated to the thermal conductivity of the evolved gas.

As a test reaction, the dehydration of calcium oxalate was chosen,

$$CaC_2O_4 \cdot H_2O\,(s) \rightarrow CaC_2O_4\,(s) + H_2O\,(g)$$

$$\Delta H_{298} = 38.1\ \text{kJ/mole}\ (25) \qquad (6)$$

The predicted weight change, $\Delta W/W$, for this reaction is 0.123. The thermal conductivity of the purge gas was controlled by utilizing mixtures of N_2 and He or Ar and He. The method of Wassiljewa (20), as modified by Mason and Saxena (21), was used to compute the thermal conductivity of these gaseous mixtures at room temperature (see Appendix). The compositions and thermal conductivities of gaseous mixtures used as the purge gas are given in Table 2. The values of the thermal conductivities (K') calculated by the mole fraction averaging method are also included. These values indicate the magnitude of the error introduced on the assumption that the thermal conductivities are additive.

DSC profiles for the dehydration of calcium oxalate for various sample weights are shown in Fig. 3. The effect of sample size on the temperature and the indicated energy change of this reaction is shown in Fig. 4. These experiments were performed using pure dry N_2 as the purge gas, at a flow rate of 31.8 ml/min, while the temperature was increased at a rate of 10°C/min. This means that the thermal conductivity of the purge gas was kept constant as the sample weight was varied from 0.7 to 3.4 mg. The effect of sample weight on the indicated enthalpy of dehydration appears to be small. However, the effect of sample size on the temperature of dehydration is substantial. When the sample weight was increased by slightly less than an order of magnitude, the dehydration temperature was observed to increase by 20°C.

The effect of thermal conductivity on the dehydration of calcium oxalate is shown in Fig. 5. The sample weight used in these studies was 1.7 mg and the flow rate and heating

TABLE 2
Thermal Conductivities of Purge Gas Mixtures Used in Calcium Oxalate Dehydration Experiments (1) Calculated Using Wassiljewa's Correlation, K, and (2) Calculated by Mole Fraction Averaging, K'

Gas composition (%)			Thermal conductivity (W/(m K))	
N_2	He	Ar	K	K'
0	10	90	0.0237	0.0304
0	8	92	0.0224	0.0278
0	6	94	0.0211	0.0252
100	0	0	0.0257	0.0257
95	5	0	0.0284	0.0318
90	10	0	0.0313	0.0379
85	15	0	0.0344	0.0440

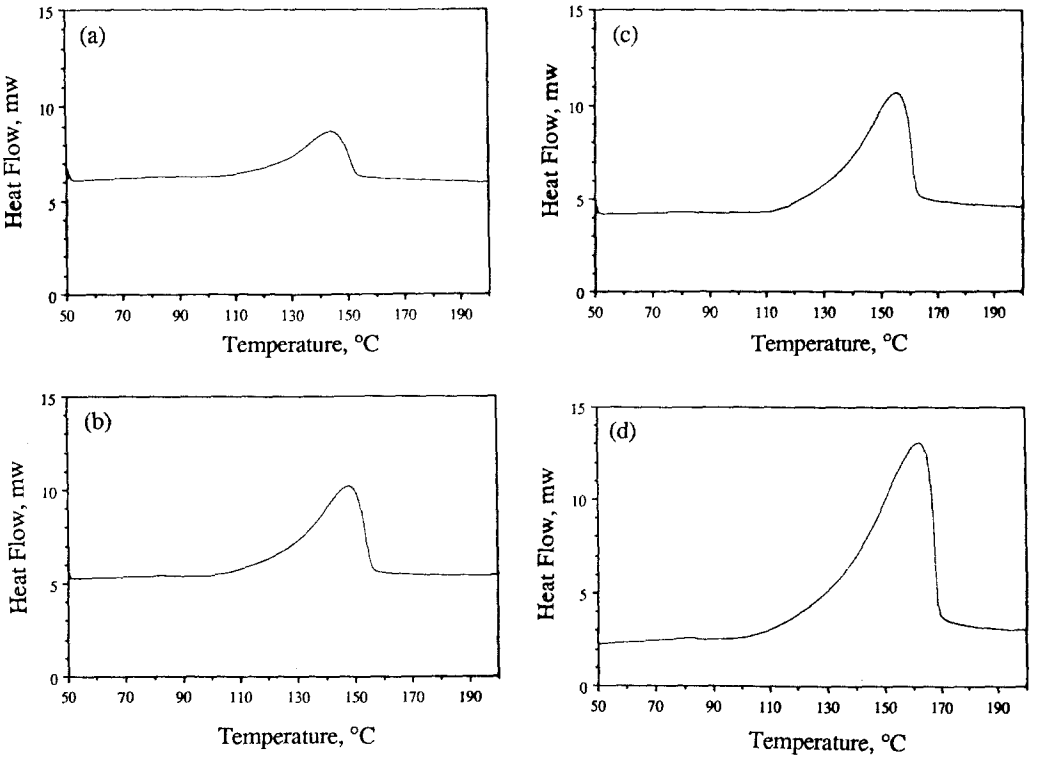

FIG. 3. DSC profiles of the dehydration of calcium oxalate at various sample weights. (a) 0.7 mg, (b) 1.6 mg, (c) 2.6 mg, (d) 3.4 mg.

rate were maintained constant at 31.8 ml/min and 10°C/min, respectively. The effect of thermal conductivity on the enthalpy of dehydration was substantial. However, the effect of thermal conductivity on the temperature of dehydration was not particularly significant.

Because several researchers (*22, 23*) have suggested that the heating rate of the sample may have a significant effect on the tempera-

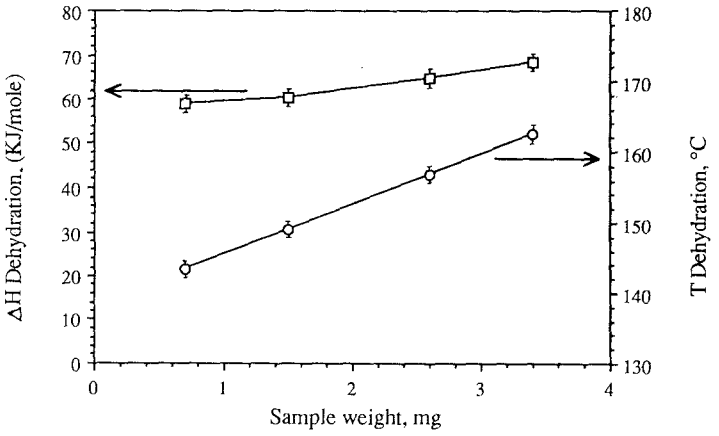

FIG. 4. The effect of sample size on the dehydration of calcium oxalate.

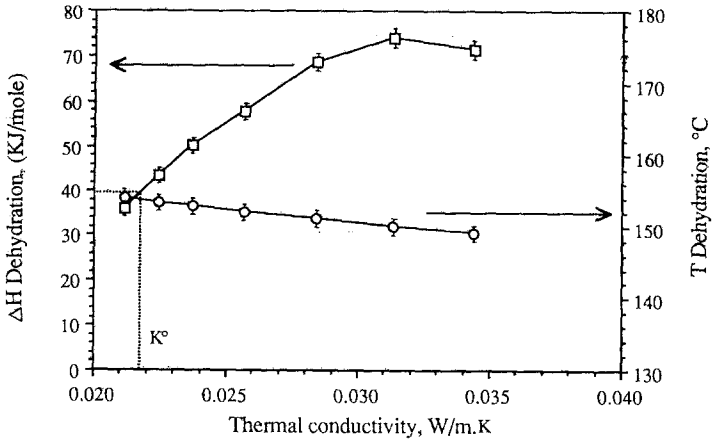

FIG. 5. The effect of purge gas thermal conductivity on the dehydration of calcium oxalate. The thermal conductivity of the H_2O boundary layer is calculated at the average temperature of solid and gas phases (70°C) as K_0.

ture of a transition, an experiment was performed to assess the importance of this variable. The results of this study, which was performed at constant thermal conductivity and at two sample sizes of 0.8 and 1.7 mg, are shown in Fig. 6. It can be observed that the dehydration temperature, T, is a significant function of the heating rate.

The effect of purge gas flow rate on the indicated enthalpy and temperature of dehydration was also studied. The results of this study are shown in Fig. 7. The sample size and heating rate chosen for this study were 1.7 mg and 10°C/min, respectively. The effect of the flow rate on the indicated enthalpy of dehydration was not significant.

We conclude from these studies that the only variable which has a significant effect on the indicated enthalpy of dehydration is the thermal conductivity of the purge gas. Accuracy in the measurement of enthalpies

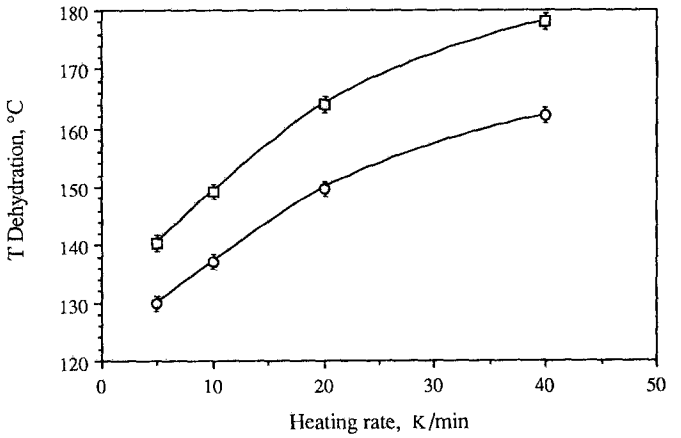

FIG. 6. The effect of heating rate on the dehydration temperature of calcium oxalate. (□) 1.7 mg, (○) 0.8 mg.

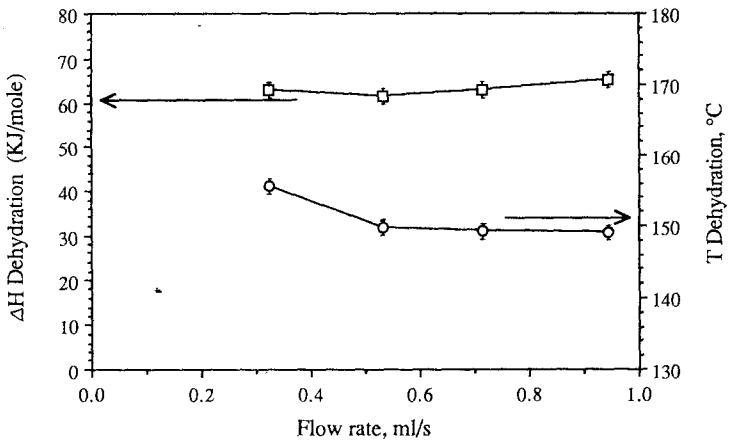

FIG. 7. The effect of purge gas flow rate on the dehydration of calcium oxalate.

of dehydration will be increased when the heating rate is greater than 10°C/min, and the sample size is less than 2 mg. However, the latter effects are secondary in comparison with the thermal conductivity of the purge gas.

In order to obtain the correct enthalpy of dehydration, the curve representing the indicated enthalpy as a function of thermal conductivity (Fig. 5) is extrapolated to the thermal conductivity of the evolved gas, namely H_2O. Although the accurate determination of the composition and temperature of this boundary layer requires a rigorous mass and heat transfer analysis, two approximate assumptions are made here. First, it is assumed that the reaction rate is high enough so that the boundary layer will consist of water only. Second, the temperature of the boundary layer is assumed to be equal to the average of the sample dehydration and purge gas temperatures. The sample dehydration temperature is determined experimentally by the double extrapolation technique outlined in Fig. 8. First, the dehydration temperatures (Fig. 6) are extrapolated to a zero heating rate for the two sample weights. This gives dehydration temperatures of 122 and 130°C for sample sizes of 0.8 and 1.7 mg, respectively. A second extrapolation corresponding to a heating rate of 0°C/min is drawn linearly, similar to that corresponding to 10°C/min. Extrapolation to a zero sample weight results in a dehydration temperature of 115°C. The temperature of the H_2O boundary layer is then calculated as the average of the solid and gas temperatures (115 and 25°C, respectively), i.e., 70°C. This results in a thermal conductivity of $K^\circ = 0.0216$ W/(m K) and the method will yield an enthalpy of dehydration of 40 ± 2 kJ/mole. Correction for the standard reference temperature of 298 K can be made by estimating the heat capacity of calcium oxalate using Kopp's rule (*24*). This correction amounts to −0.25 kJ/mole, which is well within the uncertainty margin for the reported ΔH_f values and is quite negligible. Therefore, the value obtained by this method is in excellent agreement with the literature value of 38.1 kJ/mole (*25*).

The measured weight loss ratio ($\Delta W/W$) obtained was 0.119, in good agreement with the predicted weight loss of 0.123. This agreement suggests that the dehydration reaction has gone to completion.

As an example of the second type of a gas–solid reaction, we have measured the enthalpy of reduction of PtO_2. This reduction proceeds according to the equation

$$PtO_2\,(s) + 2H_2\,(g) \rightarrow Pt\,(s) + 2H_2O\,(g)$$

$$\Delta H_{298} = -315.1 \text{ kJ/mole } (25)$$

$$\Delta H_{298} = -349.8 \text{ kJ/mole } (26) \qquad (7)$$

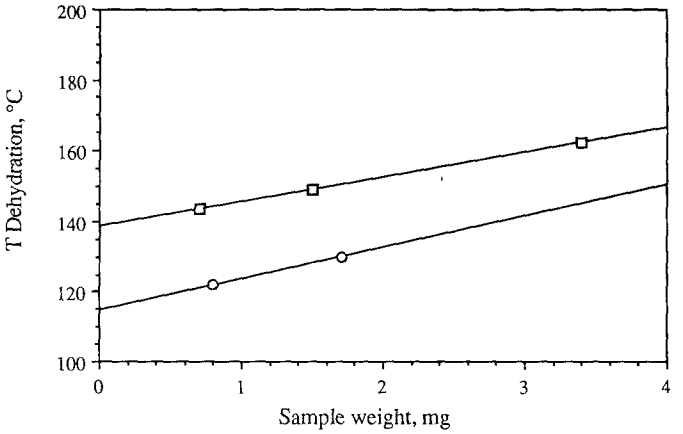

FIG. 8. Determination of the dehydration temperature of calcium oxalate by double extrapolation. (□) 10°C/min, (○) 0°C/min.

The predicted weight loss ratio of $\Delta W/W = 0.141$ is in good agreement with the experimentally determined weight loss ratio of 0.132, suggesting complete reduction to metallic Pt.

For a reduction reaction of this type, the following heat transfer effects require consideration:

(1) The evolution of gaseous products into the purge gas stream as in the case for the dehydration reaction outlined previously.

(2) Dissimilarity between the thermal resistance of the sample and the reference due to the consumption of hydrogen by the sample.

Two types of extrapolations appear necessary: First, extrapolation to the thermal conductivity of the evolved gas and second, extrapolation to zero hydrogen gas concentration. The effect of sample size is readily eliminated by taking a sample which is sufficiently small. With this in mind, two sets of experiments were designed:

(1) The enthalpy and temperature of reduction were measured while keeping the thermal conductivity constant and varying the concentration of H_2 in the Ar purge gas. The compositions of the purge gas mixtures used are shown in Table 3. Helium was used as an auxiliary gas in order to maintain the thermal conductivity constant. The constant value of the thermal conductivity was selected as that corresponding to a mixture consisting of 15% H_2 in Ar, i.e., 0.0320 W/(m K).

(2) The enthalpies and temperatures of reduction were measured as a function of thermal conductivity for constant H_2 concentrations in Ar. The thermal conductivity was varied by changing the He concentration in the purge gas. This set of experiments was performed using five different hydrogen concentrations, 0.5, 1.0, 1.5, 2.5, and 5% H_2. The compositions and thermal conductivities of these mixtures are shown in Table 4. Typical DSC profiles for the reduction of PtO_2 at a constant H_2 concentration of 5% are shown in Fig. 9.

The results of the first set of experiments which show the effect of H_2 concentration

TABLE 3

Compositions of Purge Gas Mixtures Used in Constant Thermal Conductivity (0.0320 W/(m K)) Experiments for the Reduction of PtO_2

Gas	Composition (%)						
H_2	15	10	5	2.5	1.5	1.0	0.5
Ar	85	82.7	80.4	79.2	78.8	78.5	78.3
He	0	7.3	14.6	18.3	19.7	20.5	21.2

TABLE 4

Compositions and Thermal Conductivities of Purge Gas Mixtures Used in Constant H_2 Concentration Experiments for the Reduction of PtO_2

Gas	Composition (%)		
H_2	0.5	0.5	0.5
Ar	99.5	94.5	89.5
He	0.0	5.0	10.0
K	0.0179	0.0209	0.0241
H_2	1.0	1.0	1.0
Ar	99.0	94.0	89.0
He	0.0	5.0	10.0
K	0.0183	0.0214	0.0246
H_2	1.5	1.5	1.5
Ar	98.5	93.5	88.5
He	0.0	5.0	10.0
K	0.0187	0.0218	0.0250
H_2	2.5	2.5	2.5
Ar	97.5	92.5	87.5
He	0.0	5.0	10.0
K	0.0197	0.0228	0.0260
H_2	5.0	5.0	5.0
Ar	95.0	90.0	85.0
He	0.0	5.0	10.0
K	0.0220	0.0252	0.0286

on the indicated enthalpy and temperature of reduction at constant thermal conductivity are shown in Fig. 10. At low H_2 concentrations a sharp decrease in the enthalpy of reduction is observed. These experiments were performed using a constant sample weight and thermal conductivity of 1.4 mg and 0.0320 W/(m K), respectively. The heating rate was 10°C/min and the flow rate was 31.8 ml/min. The indicated enthalpy of reduction approaches its true value at low H_2 concentrations. The temperature of reduction also approaches an asymptotic value at zero H_2 concentration. Therefore, in order to determine the temperature of reduction, extrapolation to zero H_2 concentration was performed using a least-square third-order polynomial fitting. This resulted in a reduction temperature of 82.4°C.

The effect of thermal conductivity on the indicated enthalpy and temperature of reduction for five different H_2 concentrations was studied. The results of these experiments, which were performed at constant sample size and heating rate, are shown in Figs. 11 and 12. The temperatures of reduc-

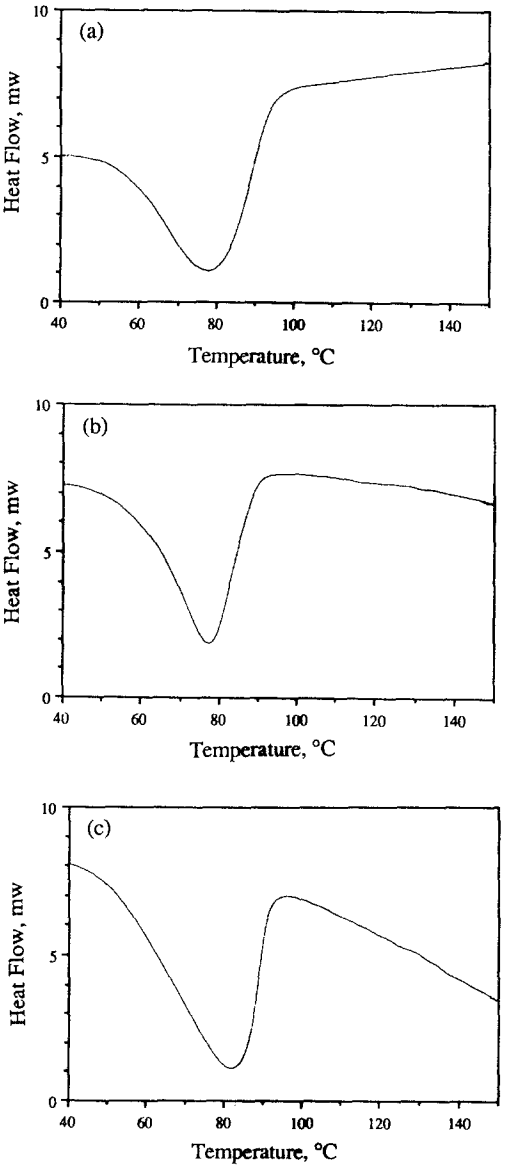

FIG. 9. DSC profiles of the reduction of PtO_2 at a constant H_2 concentration of 5% and various thermal conductivities of (a) 0.0220 W/(m K), (b) 0.0252 W/(m K), (c) 0.0286 W/(m K).

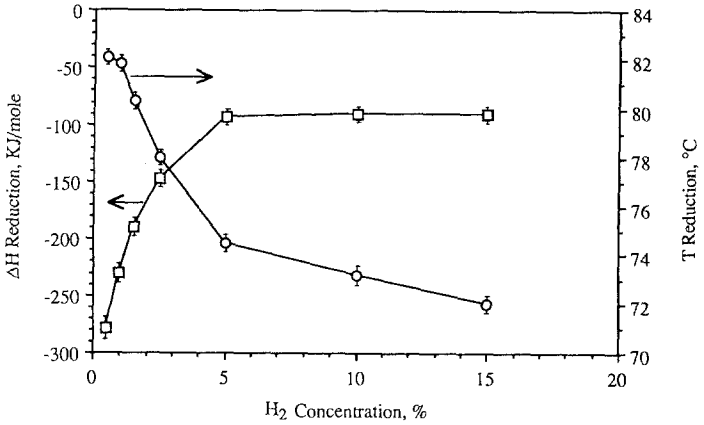

FIG. 10. The effect of H_2 concentration on the reduction of PtO_2 at constant thermal conductivity of the purge gas (0.0320 W/(m K)).

tion do not show a systematic variation with respect to thermal conductivity. For this reason T_r was determined by extrapolation to zero H_2 concentration, as determined previously (Fig. 10).

The temperature of the H_2O boundary layer was calculated as the average of the solid- and gas-phase temperatures as in the previous case. This resulted in a temperature of 53.7°C. The linear interpolations (extrapolation in the case of 5% H_2 concentration) of the indicated enthalpies of reduction to the thermal conductivity of the evolved gas at the temperature of the H_2O boundary layer (0.0199 W/(m K) at 53.7°C) gave five values corresponding to the five different H_2 concentrations (Fig. 11). These enthalpy values were plotted as a function of H_2 concentration. Extrapolation to zero concentration yielded the true value of the enthalpy of reduction. A least-square second-order polynomial curve fitting was used for this extrapolation. The results of this plot, shown in Fig. 13, yield an enthalpy of reduc-

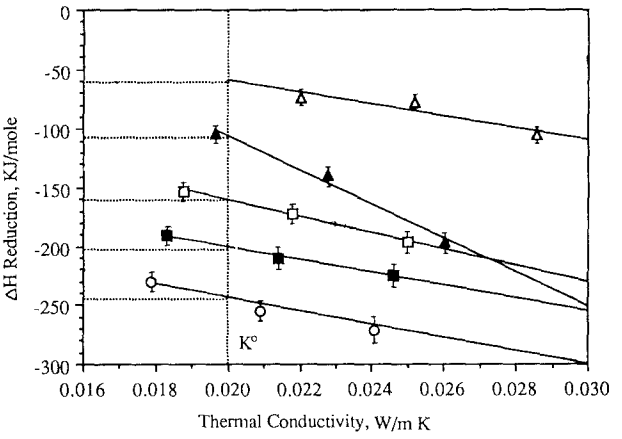

FIG. 11. The effect of purge gas thermal conductivity on the enthalpy of the reduction of PtO_2 at different H_2 concentrations. (○) 0.5% H_2, (■) 1.0% H_2, (□) 1.5% H_2, (▲) 2.5% H_2, (△) 5% H_2.

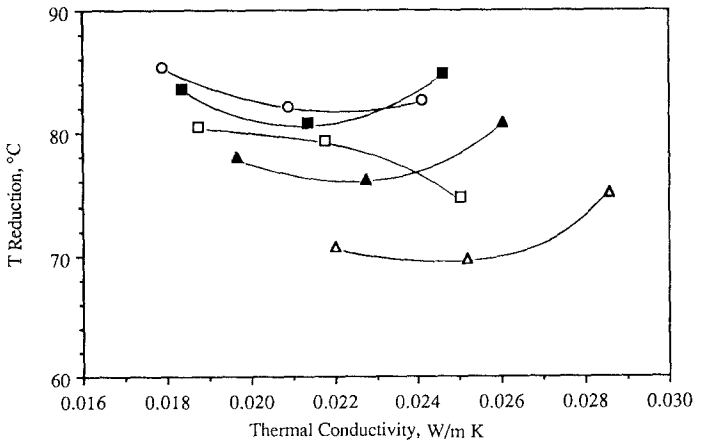

FIG. 12. The effect of purge gas thermal conductivity on the temperature of the reduction of PtO_2 at different H_2 concentrations. (○) 0.5% H_2, (■) 1.0% H_2, (□) 1.5% H_2, (▲) 2.5% H_2, (△) 5% H_2.

tion of -295 ± 13 kJ/mole. This value can be corrected for the reference temperature of 298 K by using the appropriate heat capacity data (*25*). This correction amounts to 13.3 kJ/mole. Thus the final enthalpy value of -281.7 ± 13 kJ/mole is in reasonable agreement with the lower literature value of -315.1 kJ/mole (*25*).

One final reduction reaction was performed in order to test the validity of the method. The reduction of $PtCl_2$ in H_2 proceeds according to

$$PtCl_2(s) + 2H_2(g) \rightarrow Pt(s) + 2HCl(g)$$

$$\Delta H_{298} = -35.6 \text{ kJ/mole } (25)$$

$$\Delta H_{298} = -66.1 \text{ kJ/mole } (26). \quad (8)$$

The experimental weight loss of $\Delta W/W = 0.285$ was in good agreement with the predicted weight loss $\Delta W/W = 0.268$. The experiments were carried out by a method which was identical to that used for the reduction of PtO_2. The results of these experiments are shown in Figs. 14 to 16. A final extrapolated value of the enthalpy of reduction, $\Delta H = -67 \pm 3.5$ kJ/mole, was obtained at a reduction temperature of 58.3°C. This enthalpy is in reasonable agreement with the literature value of -66.1 kJ/mole (*26*). The heat capacity correction for this reaction was found to be negligible, due to the low temperature of reduction.

A summary of the experimental results of the enthalpies of selected gas–solid reactions is shown in Table 5, along with the corresponding literature values. It should be noted that experimental data for standard enthalpies of formation are not only scarce in the literature but, as in the case of reduction of $PtCl_2$, large discrepancies exist.

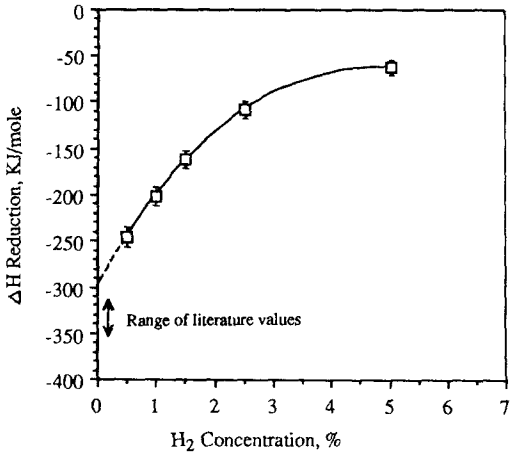

FIG. 13 The combined effect of H_2 concentration and purge gas thermal conductivity on the enthalpy of the reduction of PtO_2.

TABLE 5

Summary of Results: Enthalpy of Gas–Solid Reactions by DSC

Reaction	Enthalpy (kJ/mole)		
	Literature[a]	Literature[b]	Experimental
CaC_2O_4 dehydration	—	38.1	39 ± 1
PtO_2 reduction	−349.8	−315.1	−297 ± 15
$PtCl_2$ reduction	−66.1	−35.6	−62 ± 3

[a] Ref. (*26*).
[b] Ref. (*25*).

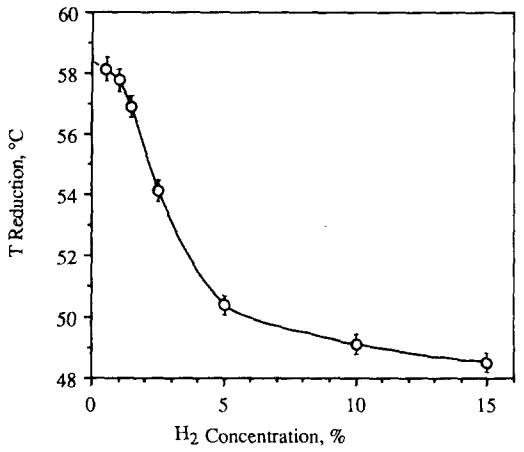

FIG. 14. The effect of H_2 concentration on the reduction temperature of $PtCl_2$ at constant thermal conductivity of the purge gas (0.0320 W/(m K)).

CONCLUSIONS

This study shows the significance of experimental operating conditions or "artifacts" in thermal analysis, which have been overlooked or avoided by most researchers. Quantitative analysis is possible only when important variables are identified and their optimum values are approached.

The extrapolation technique presented here should be applicable to various gas–solid reactions of interest in different fields. This technique will provide a quick estimate of the enthalpy and will be useful when heat of formation values are not available. Selection of a purge gas with a thermal conductivity in the vicinity of the product gas will enhance the accuracy. In a future

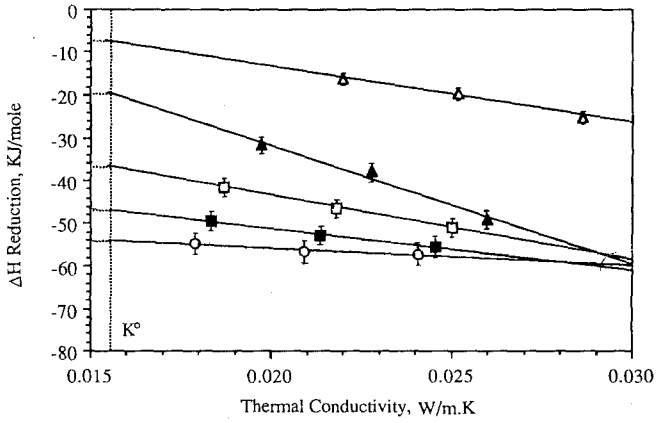

FIG. 15. The effect of purge gas thermal conductivity on the enthalpy of the reduction of $PtCl_2$ at different H_2 concentrations. (○) 0.5% H_2, (■) 1.0% H_2, (□) 1.5% H_2, (▲) 2.5% H_2, (△) 5% H_2.

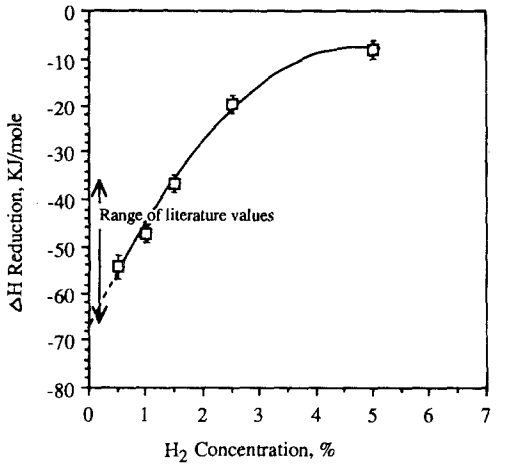

FIG. 16. The combined effect of H_2 concentration and purge gas thermal conductivity on the enthalpy of the reduction of $PtCl_2$.

study this technique will be utilized in the identification of reduction steps and intermediates of metallic catalyst precursors.

APPENDIX

Calculation of Thermal Conductivity of a Gaseous Mixture

According to Wassiljewa (*20*) the thermal conductivity of a gas mixture, λ_m, can be calculated by the empirical equation

$$\lambda_m = \sum_{i=1}^{n} \frac{y_i \lambda_i}{\sum_{j=1}^{n} y_i A_{ij}},$$

where y_i = mole fraction of component i; A_{ij}'s are binary parameters which can be expressed according to Mason and Saxena (*21*) by

$$A_{ij} = \frac{[1 + (\lambda_{tr_i}/\lambda_{tr_j})^{1/2}(M_i/M_j)^{1/4}]^2}{[8(1 + M_i/M_j)]^{1/2}};$$

and $A_{ii} = 1$. Here, M is the molecular weight and λ_{tr} is the monatomic value of thermal conductivity which can be calculated from viscosity values of η_i and η_j:

$$\frac{\lambda_{tr_i}}{\lambda_{tr_j}} = \frac{\eta_i}{\eta_j}\frac{M_j}{M_i}.$$

Since η depends on temperature and pressure, A_{ij}'s will also be a function of T and P. All thermal conductivities of gaseous mixtures used in this study are calculated according to the above correlations. Experimental data reported (*27*) agree well with the predictions of these correlations.

ACKNOWLEDGMENTS

The authors acknowledge support from the U.S. Department of Energy (Grant DOEFG02-86ER-1351) for this research. We also thank Amoco Corp. for an equipment grant which was made available to us.

REFERENCES

1. Chou, P., and Vannice, M. A., *J. Catal.* **104,** 1 (1987).
2. Muller, B. W., and Boeke, A. W., *Pharm. Weekbl.* **113,** 941 (1978).
3. Thompson, D. S., *in* "Thermal Analysis" (R. F. Schwenker, Jr., and P. D. Garn, Eds.), Vol. 2. Academic Press, New York/London, 1969.
4. Hirano, K., *in* "Thermal Analysis: Comparative Studies in Materials" (H. Kambe and P. D. Garn, Eds.). Wiley, New York, 1974.
5. Yinnon, H., and Uhlman, D. R., *J. Non-Cryst. Solids* **54,** 253 (1983).
6. Bansal, N. P., Bruce, A. J., Doremus, R. H., and Moynihan, C. T., *J. Non-Cryst. Solids* **70,** 379 (1985).
7. Watson, E. S., O'Neill, M. J., Justin, J., and Brenner, N., *Anal. Chem.* **36**(7), 1233 (1964).
8. Van Dooren, A. A., and Muller, B. W., *Thermochim. Acta* **49,** 151 (1981).
9. De Bruijn, C. M. A., and Marel, V. D., *Geol. Mijnbouw*, 69 (1954).
10. Boersma, S. L., *J. Amer. Ceram. Soc.* **38,** 281 (1955).
11. Ozawa, T., *Bull. Chem. Soc. Japan* **39,** 2071 (1966).
12. Flynn, J. H., *in* "Status of Thermal Analysis" (O. Menis, Ed.), pp. 119–136. NBS Special Publication 338, US Government Printing Office, Washington DC, 1970.
13. Saito, Y., Saito, K., and Atake, T., *Thermochim. Acta* **107,** 277 (1986).
14. Stone, R. L., *Anal. Chem.* **32**(12), 1582 (1960).
15. Vold, M. J., *Anal. Chem.* **21,** 683 (1949).
16. Borschardt, H. J., and Daniels, F., *J. Amer. Chem. Soc.* **79,** 41 (1957).
17. Reed, R. L., Weber, L., and Gottfried, B. S., *Ind. Eng. Chem. Fundam.* **4,** 38 (1965).
18. Gray, A. P., *in* "Analytical Calorimetry" (R. S.

Porter and J. F. Johnson, Eds.), Vol. 2, pp. 209–218. Plenum, New York, 1968.
19. Reid, R. C., Prausnitz, J. M., and Poling, B. E., The Properties of Gases and Liquids, 4th Ed., p. 515. McGraw–Hill, New York, 1987.
20. Wassiljewa, A., *Phys. Z.* **5,** 737 (1904).
21. Mason, E. A., and Saxena, S. C., *J. Chem. Phys.* **28,** 623 (1958).
22. Barral, E. M., and Rogers, L. B., *J. Inorg. Nucl. Chem.* **28,** 41 (1966).
23. Langer, A. M., and Kerr, P. F., *Amer. Mineral.* **52,** 509 (1967).
24. Thompson, E. V., and Ceckler, W. H., Introduction to Chemical Engineering, p. 64. McGraw–Hill, New York, 1977.
25. Karapetyants, M. Kh., and Karapetyants, M. L., Thermodynamic Constants of Inorganic and Organic Compounds, pp. 213–214. Ann Arbor Science Publishers, Ann Arbor, MI, 1970.
26. Weast, R. C., and Astle, M. J., CRC Handbook of Chemistry and Physics, pp. D67–D77. CRC Press, Boca Raton, FL, 1979.
27. Touloukian, Y. S., Liley, P. E., and Saxena, S. C., Thermal Conductivity: Non-metallic Liquids and Gases, pp. 295–381. IFI/Plenum, New York, 1970.